Capacitive-mesh output couplers for optically pumped far-infrared lasers

D. A. Weitz, W. J. Skocpol, and M. Tinkham

Department of Physics and Division of Applied Sciences, Harvard University, Cambridge, Massachusetts 02138
Received March 15, 1978

The use of capacitive-mesh output couplers for optically pumped far-infrared molecular lasers has been extended throughout the far-infrared spectrum, between 42 μm and 1.2 mm, and the optimum grid constants have been found for several lines. At shorter wavelengths, performance has been improved by the use of a novel hybrid capacitive-mesh hole output coupler.

The performance of optically pumped far-infrared (FIR) molecular lasers has recently been substantially improved by the use of overmoded dielectric waveguide cavities.[1-3] In order to take full advantage of the favorable characteristics of these lasers, it is important to use a well designed output coupling mirror, a component that has received much attention recently. This mirror should have high reflectivity at the pump wavelength, λ_p, and partial reflectivity and low absorptivity at the FIR wavelength, λ_{FIR}, and should couple out over a broad area of the laser mode to limit diffraction. Among the schemes that have been used to meet these requirements are hybrid metal-mesh dielectric (MMD) mirrors,[4,5] hybrid metal dielectric hole (MDH) couplers,[1,2] etalons,[1,5,6] and capacitive-mesh couplers.[7] This Letter reports on the extension of the use of capacitive-mesh couplers throughout the FIR spectrum and the use of a novel hybrid capacitive-mesh hole coupler for improved performance at shorter FIR wavelengths.

We have chosen to use capacitive-mesh couplers because of the relative simplicity and low cost of their fabrication compared with the devices used in the other schemes. Unlike etalons, the substrate thickness does not have to be finely adjusted; unlike MMD couplers, their fabrication does not require photolithographic masking techniques; and unlike MMD and MDH couplers, they do not require a dielectric reflection coating for the pump radiation. The capacitive mesh itself meets the reflectivity requirements at both the pump and the FIR wavelengths. The mesh period, g [see Fig. 1(a)], is comparable to λ_{FIR} for partial FIR transmission[8] but is much greater than λ_p for reasonably high reflectivity of the 10-μm pump radiation. The high reflectivity at λ_p permits the use of a crystal-quartz substrate, which is strongly absorbing at 10 μm, eliminating the necessity of filtering any remaining pump power from the output. It also removes the need for a dielectric coating, reducing the FIR absorption losses, which can otherwise become quite severe for $\lambda_{FIR} \lesssim 100$ μm.[2] Finally, if different values of g are used, the FIR feedback at any given λ_{FIR} can be relatively finely tuned.

In our experimental setup, pump power was supplied by a modified commercial CO_2 laser[9] that had a 12-mm-diameter, 1.8-m-long cavity, whose active region was enclosed by two ZnSe Brewster-angle windows. It was tuned by a 75 line/mm grating and had a 20-m radius-of-curvature output coupler mounted on a PZT stack for fine frequency tuning. Output couplers with reflectivities of 36 and 65% were used for the stronger and weaker CO_2 lines, respectively, and gave at least 15 W in an output mode reasonably close to Gaussian, for efficient coupling to the FIR cavity.[2] The FIR cavity was a 38-mm-diameter, 3-m-long dielectric waveguide[1] made with Pyrex industrial pipe. An $\sim f/50$ mirror was used to focus the CO_2 beam into the cavity through a BaF_2 vacuum window and a 3-mm-diameter center coupling hole in a flat mirror mounted on a translation

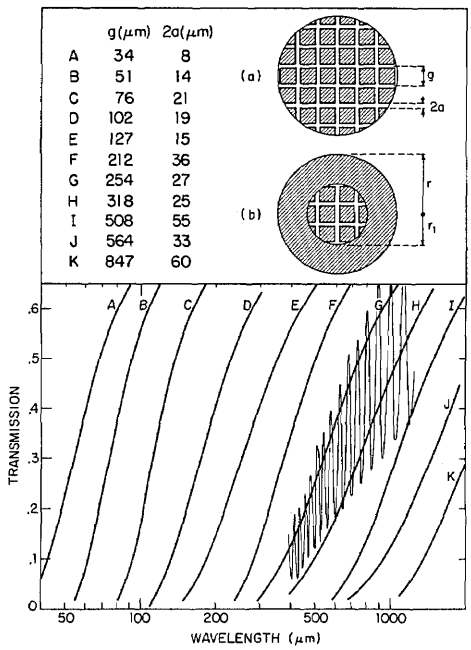

Fig. 1. Calculated transmission of capacitive meshes on crystal quartz as functions of wavelength. The thin line shows the etalon effects for mesh G on a 2-mm-thick quartz substrate. The inset on the upper right shows schematically (a) a capacitive-mesh output coupler and (b) a hybrid capacitive-mesh hole coupler.

0146-9592/78/0700-0013$0.50/0

stage for tuning the cavity. The capacitive-mesh output coupler served both as the other mirror and the other vacuum window of the FIR cavity.

The capacitive-mesh couplers were made on 2-mm-thick, z-cut crystal-quartz substrates, optically polished on both sides. A horizontal inductive mesh (the complementary structure to the capacitive mesh)[10] of the appropriate g served as both the support and the mask for the substrate, while about 300 nm of Al was vacuum deposited from below to form the capacitive mesh. Al was used for both its low cost and good adhesion; the substrates could be used repeatedly (they were easily cleaned in a solution of KOH in water), and the masks could be used for several evaporations. Attempts to use Au were much less successful, as shadowing effects led to poorly defined mesh structure.

Figure 1 shows the calculated[8] FIR transmission of various capacitive meshes as functions of wavelength. The mesh is assumed to be on an (infinite) crystal-quartz substrate, and absorption losses have been neglected. The exact transmission will be influenced by substrate etalon effects,[7] as shown by the thin line in Fig. 1, which is the calculated transmission of mesh G on a 2-mm-thick quartz substrate. In those cases where the thickness of the substrate is known to sufficient accuracy, the calculated transmissions are in good agreement with those measured experimentally. For example, at 496 μm, the measured transmission of the substrate and mesh with $g = 318$ μm was ~10%, while the calculated value was ~7%. On the same substrate, a mesh with $g = 254$ μm had a measured transmission of ~25% compared with the calculated value of ~24%. The use of a plot similar to Fig. 1 that included all the available electroformed meshes[10] suitable for masks was helpful as a guide in the initial determination of appropriate g and $2a$ for a given λ_{FIR}. If more than one mesh giving the required transmission was available, $g/2a$ was chosen to maximize the area covered by metal, to improve the λ_p reflectivity. Because they were so simple to fabricate, a number of different mirrors could easily be tested to determine experimentally the optimum mesh constants.

We have used capacitive-mesh couplers throughout the FIR spectrum, from 42 μm to 1.2 mm. Table 1 lists the laser lines we have tried with the mesh constants that have worked at those wavelengths. When several different meshes were used for the same line, the values of g and $2a$ for the output coupler that gave the best performance are underlined. Optimizing the FIR transmission within the range of ~(5–50)% can increase the output power by ~(20–50)%. For example, changing g from 318 to 254 μm increased the 496-μm output power by ~25%. The stronger lines (e.g., 119 μm) will lase even when they are severely undercoupled or overcoupled, but the output power is decreased by over an order of magnitude. This list is not meant to show all the unoptimized values of g that will work for each line. The highest FIR output power is obtained with the laser operating in the favorable, linearly polarized, single-peak EH_{11} mode.[11] Using the optimized mesh constants, we obtain typical output powers of ~10 mW at 496 μm and ~80 mW at 119 μm with ~17–20-W pump power. We have made some preliminary comparisons with MDH couplers at a number of λ_{FIR} and find that the total output power seems to be approximately the same (to within ~50%). However, changing the grid constants of the capacitive-mesh couplers gave finer control of the reflectivity over the central portion of the coupler and permitted better optimization and improved performance for some λ_{FIR}. Of course, the diffractive divergence of the output beam is reduced with the capacitive-mesh couplers.

For $\lambda_{FIR} < 100$ μm, it was necessary to use a hybrid capacitive-mesh hole coupler to obtain good laser performance. A second evaporation produced a ring-shaped Al mirror and left a center hole of radius r_1 covered only with the appropriate capacitive mesh, as shown schematically in Fig. 1(b). This not only increased the FIR feedback but also considerably improved the CO_2 reflectivity, which drops off substantially for the mesh constants necessary for these λ_{FIR}. At 70.5 μm, the best performance was obtained with $r_1 = 10$ mm (compared with $r = 19$ mm for the waveguide cavity) and a mesh with $g = 51$ μm. Figure 2 shows a spatial scan across the output beam of the mode with the highest output power, the EH_{11} mode. The far-field intensity of the EH_{11} mode, coupled out through a hole with $r_1 < r$, can be shown to be

$$I \propto \left\{ \frac{1}{A^2 - (Br_1)^2} [AJ_1(A)J_0(Br_1) - Br_1J_0(A)J_1(Br_1)] \right\}^2, \quad (1)$$

Table 1. Mesh Constants for FIR Wavelengths

λ_{FIR} (μm)	Gas	Pump Line	$g(2a)$ (μm; Best Values Underlined)
41.7	CH_3OH	9P(32)	34(7.6)[a]
70.5	CH_3OH	9P(34)	34(7.6),[b] <u>51(14)</u>[c]
118.8	CH_3OH	9P(36)	34(7.6), 51(14), <u>76(21)</u>, 318(25)
148.5	CH_3NH_2	9P(24)	<u>76(21)</u>, 254(27)
170.6	CH_3OH	9P(36)	<u>76(21)</u>, 318 (25)
202.4	CH_3OH	9P(36)	76(21)
233.9	N_2H_4	10R(8)	<u>212(36)</u>, 254(27)
415	CH_2CF_2	10P(14)	847(60)
496.1	$^{12}CH_3F$	9P(20)	<u>254(27)</u>, 318(25)
554.4	CH_2CF_2	10P(14)	847(60)
890.0	CH_2CF_2	10P(22)	847(60)
1221.8	$^{13}CH_3F$	9P(32)	564(33), <u>847(60)</u>

[a] Hybrid—$r_1 = 3$ mm. [b] Hybrid—$r_1 = 8$ mm. [c] Hybrid—$r_1 = 10$ mm.

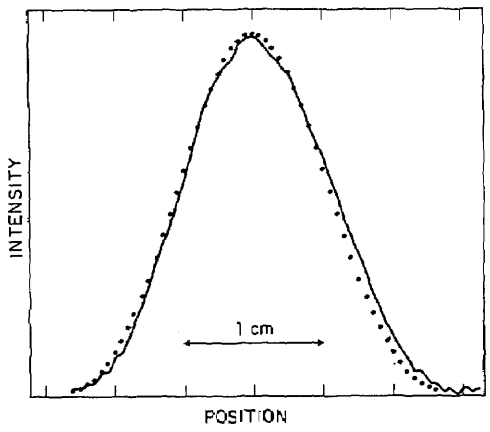

Fig. 2. Scan across the output of the strongest mode at 70.5 μm, using a 20-mm-diameter hybrid capacitive-mesh hole output coupler with $g = 51$ μm. The detector had an aperture of 1 mm and was 3.17 m away from the laser. The dots are the calculated far-field pattern from Eq. (1) in the text and are scaled only to the peak intensity.

with $A = u_{01}r_1/r$ and $B = 2\pi \sin\theta/\lambda$. J_0 and J_1 are the first and second Bessel functions, u_{01} is the first zero of J_0, and $\sin\theta$ is the angular displacement. The solid dots in Fig. 2, the calculated far-field intensities using Eq. (1), are in excellent agreement with the data. Equation (1) can also be used to calculate the half-angle divergence at the e^{-2} point,

$$\theta_c = f(r_1/r)\lambda/r_1, \tag{2}$$

where $f(r_1/r)$ must be evaluated. The two limiting values of f for a given r_1 are $f(r \gg r_1) \approx 0.24$, in which case the intensity across the hole is uniform and the divergence is minimized, and $f(r = r_1) \approx 0.54$, in which case the intensity is peaked in the center and the divergence is maximized. In our case, $f(r_1/r = 0.52) \approx 0.43$, so that for $\lambda_{FIR} = 70.5$ μm, the predicted θ_c is 3.0 mrad, which is exactly what is measured experimentally.

The mirror quality of the capacitive mesh at λ_p is limited by both diffraction and absorption because the surface is not completely covered with metal. Both of these problems become less severe as g increases. For example, we measure the specular reflection of the capacitive-mesh coupler with $g = 254$ μm to be ~85% at λ_p. For very small g, the reflectivity at λ_p is improved by the addition of the Al ring. The amount of CO_2 radiation that leaks through the mesh to be absorbed in the quartz substrate sets a limit on the maximum pump power that can be used without breaking the mirror. However, we have had no breakage problems using ~15–20-W pump power at the shorter λ_{FIR} (small g) and over 50 W at the longer λ_{FIR} (large g).

In summary, capacitive-mesh output couplers have high reflectivity at λ_p and partial reflectivity and low absorption at λ_{FIR} and couple out the full diameter of the FIR output. They are thus well suited as inexpensive and easy-to-fabricate output mirrors for optically pumped FIR lasers.

We would like to thank D. T. Hodges, with whom we had numerous helpful discussions. Helpful suggestions were also made by S. M. Wolfe and T. A. DeTemple. This work was supported by the Joint Services Electronics Program and the Office of Naval Research, with additional equipment funds from the National Science Foundation. The research of D. A. Weitz was supported by a graduate scholarship from the National Research Council of Canada.

References

1. D. T. Hodges, F. B. Foote, and R. D. Reel, "Efficient high-power operation of the cw far-infrared waveguide laser," Appl. Phys. Lett. **29**, 662 (1976).
2. D. T. Hodges, F. B. Foote, and R. D. Reel, "High-power operation and scaling behavior of cw optically pumped FIR waveguide lasers," IEEE J. Quantum Electron. **QE-13**, 491 (1977).
3. T. A. DeTemple and E. J. Danielewicz, "Continuous-wave CH_3F waveguide laser at 496 μm: theory and experiment," IEEE J. Quantum Electron. **QE-12**, 40 (1976).
4. E. J. Danielewicz, T. K. Plant, and T. A. DeTemple, "Hybrid output mirror for optically pumped far-infrared lasers," Opt. Commun. **13**, 366 (1975).
5. M. R. Schubert, M. S. Durschlag, and T. A. DeTemple, "Diffraction-limited cw lasers," IEEE J. Quantum Electron. **QE-13**, 455 (1977).
6. K. M. Evenson, D. A. Jennings, F. R. Peterson, J. A. Mucha, J. J. Jimenez, R. M. Charlton, and C. J. Howard, "Optically pumped FIR lasers: frequency and power measurements and laser magnetic resonance spectroscopy," IEEE J. Quantum Electron. **QE-13**, 442 (1977).
7. S. M. Wolfe, K. J. Button, J. Waldman, and D. R. Cohn, "Modulated submillimeter laser interferometer system for plasma density measurements," Appl. Opt. **15**, 2645 (1976).
8. R. Ulrich, "Far-infrared properties of metallic mesh and its complementary structure," Infrared Phys. **7**, 37 (1967); R. Ulrich, K. F. Renk, and L. Genzel, "Tunable submillimeter interferometers of the Fabry–Perot type," IEEE Trans. Microwave Theory Tech. **MTT-11**, 363 (1963).
9. Apollo Lasers Model 550L.
10. Buckbee Mears Co., St. Paul, Minn. The range of meshes available is sufficient to give useful values of g and $2a$ at all wavelengths in the FIR.
11. J. J. Degnan, "Waveguide laser mode patterns in the near and far field," Appl. Opt. **12**, 1026 (1973).